

**Problem of inflation in nonlinear multidimensional cosmological models**

Tamerlan Saidov\* and Alexander Zhuk†

*Astronomical Observatory and Department of Theoretical Physics, Odessa National University,  
2 Dvoryanskaya Street, Odessa 65082, Ukraine*

(Received 7 October 2008; published 27 January 2009)

We consider a multidimensional cosmological model with nonlinear quadratic  $R^2$  and quartic  $R^4$  actions. As a matter source, we include a monopole form field, a D-dimensional bare cosmological constant and the tensions of branes located at fixed points. In the spirit of the universal extra dimension model, the standard model fields are not localized on branes, but rather they can move in the bulk. We define conditions that ensure stable compactification of the internal space in zero minima of the effective potentials. Such effective potentials may have a rather complicated form with a number of local minima, maxima, and saddle points. We investigate inflation in such models. It is shown that the  $R^2$ - and  $R^4$  models can produce up to 10 and 22 e-foldings, respectively. These values are not sufficient to solve the homogeneity and isotropy problem, but they are large enough to explain recent cosmic microwave background data. Additionally, the  $R^4$  model can provide conditions for eternal topological inflation. The main drawback of the obtained inflationary models consists in a spectral index  $n_s$  that is less than the presently observed  $n_s \approx 1$ . For the  $R^4$  model we find, e.g.,  $n_s \approx 0.61$ .

DOI: 10.1103/PhysRevD.79.024025

PACS numbers: 04.50.-h, 11.25.Mj, 98.80.-k

**I. INTRODUCTION**

Recently, the concept of inflation has achieved spectacular success in explaining the acoustic peak structure seen in cosmic microwave background (CMB) data (cf. e.g., [1]). It is very difficult to correctly explain the large-scale structure formation of the observable part of the Universe without taking into account a stage of early inflation. Although the number of different inflation models is quite large, a basic ingredient of these models is the presence of a scalar field that moves in a background potential. Usually, the origin of the scalar field and the form of its potential remain out of the scope of corresponding investigations. An explanation of the presence of scalar fields is naturally provided by higher-dimensional theories where they arise as geometrical moduli (radions, gravexcitons), which characterize the shape of the internal spaces (acting as scale factors of the internal spaces). After dimensional reduction to four dimensions, the scalar field potential is completely defined by the topology and matter content of the original higher-dimensional model [2,3]. Therefore, it is of highest interest to clarify whether inflation can be realized in these models.<sup>1</sup>

On the other hand, scalar fields with corresponding potentials naturally originate from nonlinear gravitational models where Lagrangians  $L$  are functions of scalar curvature:  $L \propto f(R)$ . It is well known that such models are equivalent to linear-curvature models with additional scalar fields. These scalar fields correspond to additional

degrees of freedom of nonlinear models. The motivation for considering such higher-order curvature theories is comprehensively discussed in Ref. [8]. Compared, e.g., to others higher-order gravity theories,  $f(R)$  theories are not only free of ghosts and of Ostrogradski instabilities [9]. Rather these theories are very attractive because they usually contain scalar field potentials that are capable for inducing the required late-time acceleration of our Universe as an interesting alternative to a cosmological constant (see, e.g., [8,10,11] and references therein). Moreover, these theories can provide a stage of early inflation for four-dimensional setups (see, e.g., the pioneering paper by Starobinsky [12] and numerous references in [8,10]) as well as for multidimensional [11,13,14] ones.

In our paper we combine both of these approaches, i.e., we consider multidimensional models with nonlinear action functionals. We start from the simplest linear multidimensional model and show that such a model can provide power-law inflation. Unfortunately the given solution branch corresponds to a decompactified internal space.<sup>2</sup> In order to obtain inflation of the external space with subsequent stabilization of the internal spaces, we

<sup>2</sup>Considering multidimensional cosmological models we must always ensure that the internal spaces remain stabilized (quasistatically compactified) at sufficiently small scales so that they neither blow up to large scales (in conflict with observations) nor collapse to ultrasmall quantum gravity scales (where our phenomenological techniques break down). Moreover, if such a quasistatical stabilization was absent we would be confronted with a variation of the four-dimensional fundamental constants. A general phenomenological approach for stabilizing the internal space was developed in [3] and subsequently applied to numerous models. In the present paper, we follow this approach as well.

\*tamerlan-saidov@yandex.ru

†zhuk@paco.net

<sup>1</sup>For corresponding discussions and further references on string-induced inflation see, e.g., [4–6]. Similar topics for multidimensional cosmological models are considered in Ref [7].

further turn to multidimensional nonlinear models with quadratic and quartic scalar curvature nonlinearities. Starting from stability conditions for the internal spaces (quasistable compactification) we analyze the arising effective potentials as possible candidates for inflaton potentials providing inflation of the external space. We show that in the quadratic and quartic models we can achieve 10 and 22 e-folds, respectively. These numbers are sufficient to explain the present day CMB data, but they are not sufficiently large to solve the horizon and flatness problems. However, 22 e-foldings is a rather big number to encourage the present investigation of the nonlinear multidimensional models and to find theories where this number will approach 50–60 e-folds. Even more, this number (50–60) can be reduced in models with a long intermediate matter dominated stage where this latter stage immediately follows inflation (with subsequent decay into radiation). Precisely this scenario takes place for our models, where we find that the e-folds can be reduced by 6 if the mass of the decaying scalar field is of order of  $m \sim 1$  TeV. Therefore, we believe that the number of e-folds is not a big problem for the proposed models. The main problem consists in the spectral index  $n_s \approx 0.61$  (for the quartic model), which is less than the observed  $n_s \approx 1$ . A possible solution of this problem may consist in a more general form of the nonlinearity  $f(R)$ . For example, it was observed in [15] that a simultaneous consideration of quadratic and quartic nonlinearities can flatten the effective potential. We postpone the investigation of this question to one of our next papers.

To conclude, we would like to indicate two interesting features of the models under consideration. Firstly, the quartic model can provide topological inflation. Here, due to quantum fluctuations of the scalar fields, the inflating domain wall has a fractal structure (the inflating domain wall will contain a number of new inflating domain walls and each such domain wall will contain again new inflating walls, etc. [16]). So, we arrive at the so-called eternal inflation. Secondly, the obtained solution has the property of a self-similarity transformation (see Appendix B). This means that in the case of a zero minimum of the effective potential and fixed positions of the extrema in the  $(\varphi, \phi)$  plane, the change of the height of the extrema results in a rescaling of the dynamical characteristics of the model (the graphics of the number of e-folds, the scalar fields, the Hubble parameter, and the acceleration parameter versus synchronous time) along the time axis. A decrease (increase) of height by a factor  $c$  ( $c$  is a constant) leads to a stretching (shrinking) of these figures along the time axis by a factor  $\sqrt{c}$ .

The paper is structured as follows. In Sec. II, we consider an  $R$ -linear model. Nonlinear quadratic  $R^2$  and quartic  $R^4$  models are investigated in Secs. III and IV, respectively. There, we obtain the parameter ranges of stabilized internal spaces, and we investigate the possibil-

ity for inflation of the external space. A brief discussion of the obtained results is presented in the concluding Sec. V. In Appendix A, the Friedmann equations for multi-component-scalar-field models are reduced to a system of dimensionless first-order ordinary differential equations (ODEs). In Appendix B, we show that the dynamical characteristics (e.g., the Hubble parameter and the acceleration parameter) of the considered nonlinear models satisfy a self-similarity condition.

## II. LINEAR MODEL

To start with, let us define the topology of our models. We consider a factorizable  $D$ -dimensional metric

$$g^{(D)} = g^{(0)}(x) + L_{\text{Pl}}^2 e^{2\beta^1(x)} g^{(1)}, \quad (2.1)$$

which is defined on a warped product manifold  $M = M_0 \times M_1$ .  $M_0$  describes external  $D_0$ -dimensional space-time (usually, we have in mind that  $D_0 = 4$ ) and  $M_1$  corresponds to a  $d_1$ -dimensional internal space that is a flat orbifold<sup>3</sup> with branes in fixed points. The scale factor of the internal space depends on coordinates  $x$  of the external space-time:  $a_1(x) = L_{\text{Pl}} e^{\beta^1(x)}$ , where  $L_{\text{Pl}}$  is the Planck length.

First, we consider the linear model  $f(R) = R$  with  $D$ -dimensional action of the form

$$S = \frac{1}{2\kappa_D^2} \int_M d^D x \sqrt{|g^{(D)}|} \{R[g^{(D)}] - 2\Lambda_D\} + S_m + S_b. \quad (2.2)$$

$\Lambda_D$  is a bare cosmological constant.<sup>4</sup> In the spirit of universal extra dimension models [17], the standard model fields are not localized on the branes but can move in the bulk. The compactification of the extra dimensions on orbifolds has a number of very interesting and useful properties, e.g., breaking (super)symmetry and obtaining chiral fermions in four dimensions (see, e.g., the paper by H.-C. Cheng *et al.* in [17]). The latter property offers the possibility of avoiding the famous no-go theorem of Kaluza-Klein models (see, e.g., [18]). Additional arguments in favor of UED models are listed in [19].

Following a generalized Freund-Rubin ansatz [20] to achieve a spontaneous compactification  $M \rightarrow M = M_0 \times M_1$ , we endow the extra dimensions with a real-valued solitonic form field  $F^{(1)}$  with the action

$$S_m = -\frac{1}{2} \int_M d^D x \sqrt{|g^{(D)}|} \frac{1}{d_1!} (F^{(1)})^2. \quad (2.3)$$

<sup>3</sup>For example,  $S^1/Z_2$  and  $T^2/Z_2$ , which represent circle and square folded onto themselves due to  $Z_2$  symmetry.

<sup>4</sup>Such cosmological constant can originate from a  $D$ -dimensional form field that is proportional to the  $D$ -dimensional world volume  $F^{MN\dots Q} = (C/\sqrt{|g^{(D)}|})\epsilon^{MN\dots Q}$ . In this case, the equation of motion gives  $C = \text{const}$ , and the  $F^2$  term in action is reduced to  $(1/D!)F_{MN\dots Q}F^{MN\dots Q} = -C^2$ .

This form field is nested in  $d_1$ -dimensional factor space  $M_1$ , i.e.,  $F^{(1)}$  is proportional to the world volume of the internal space. In this case,  $(1/d_1!)(F^{(1)})^2 = \bar{f}_1^2/a_1^{2d_1}$ , where  $\bar{f}_1$  is a constant of integration [21].

Branes in fixed points contribute in action functional (2.2) in the form [22]

$$S_b = \sum_{\text{fixed points}} \int_{M_0} d^4x \sqrt{|g^{(0)}(x)|} L_b|_{\text{fixed point}}, \quad (2.4)$$

where  $g^{(0)}(x)$  is induced metric (which for our geometry (2.1) coincides with the metric of the external space-time in the Brans-Dicke frame), and  $L_b$  is the matter Lagrangian on the brane. In what follows, we consider the case where branes are uniquely characterized by their tensions  $L_{b(k)} = -\tau_{(k)}$ ,  $k = 1, 2, \dots, m$ , and  $m$  is the number of branes.

Let  $\beta_0^1$  be the internal space scale factor at the present time, and  $\bar{\beta}^1 = \beta^1 - \beta_0^1$  describes fluctuations around this value. Then, after dimensional reduction of the action (2.1) and conformal transformation to the Einstein frame  $g_{\mu\nu}^{(0)} = (e^{d_1 \bar{\beta}^1})^{-2/(D_0-2)} \bar{g}_{\mu\nu}^{(0)}$ , we arrive at effective  $D_0$ -dimensional action of the form

$$S_{\text{eff}} = \frac{1}{2\kappa_0^2} \int_{M_0} d^{D_0}x \sqrt{|\bar{g}^{(0)}|} \{R[\bar{g}^{(0)}] - \bar{g}^{(0)\mu\nu} \partial_\mu \varphi \partial_\nu \varphi - 2U_{\text{eff}}(\varphi)\}, \quad (2.5)$$

where scalar field  $\varphi$  is defined by the fluctuations of the internal space scale factor

$$\varphi \equiv \sqrt{\frac{d_1(D-2)}{D_0-2}} \bar{\beta}^1, \quad (2.6)$$

and  $G := \kappa_0^2/8\pi := \kappa_D^2/(8\pi V_{d_1})$  ( $V_{d_1}$  is the internal space volume at the present time) denotes the  $D_0$ -dimensional gravitational constant. The effective potential  $U_{\text{eff}}(\varphi)$  reads (hereafter we use  $D_0 = 4$ )

$$U_{\text{eff}}(\varphi) = e^{-\sqrt{(2d_1)/(d_1+2)}\varphi} [\Lambda_D + f_1^2 e^{-2\sqrt{(2d_1)/(d_1+2)}\varphi} - \lambda e^{-\sqrt{(2d_1)/(d_1+2)}\varphi}], \quad (2.7)$$

where  $f_1^2 \equiv \kappa_D^2 \bar{f}_1^2/a_{(0)1}^{2d_1}$  and  $\lambda \equiv -\kappa_0^2 \sum_{k=1}^m \tau_{(k)}$ .

Now, we should investigate this potential from the point of the external space inflation and the internal space stabilization. First, we consider the latter problem. It is clear that internal space is stabilized if  $U_{\text{eff}}(\varphi)$  has a minimum with respect to  $\varphi$ . The position of minimum should correspond to the present day value  $\varphi = 0$ . Additionally, we can demand that the value of the effective potential in the minimum position is equal to the present day dark energy value  $U_{\text{eff}}(\varphi = 0) \sim \Lambda_{DE} \sim 10^{-57} \text{ cm}^{-2}$ . However, it results in a very flat minimum of the effective potential, which in fact destabilizes the internal space [22]. To avoid this problem, we shall consider the case of zero minimum  $U_{\text{eff}}(\varphi = 0) = 0$ .

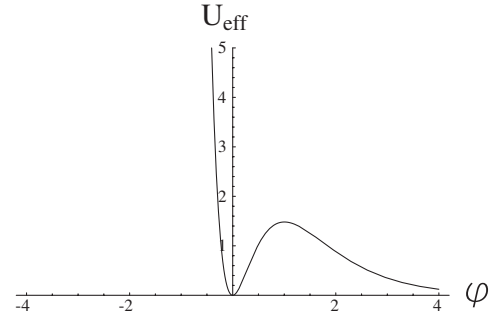


FIG. 1. The form of the effective potential (2.7) in the case  $d_1 = 3$  and  $\Lambda_D = f_1^2 = \lambda/2 = 10$ .

The extremum condition  $dU_{\text{eff}}/d\varphi|_{\varphi=0} = 0$  and zero-minimum condition  $U_{\text{eff}}(\varphi = 0) = 0$  result in a system of equations for parameters  $\Lambda_D$ ,  $f_1^2$ , and  $\lambda$ , which has the following solution:

$$\Lambda_D = f_1^2 = \lambda/2. \quad (2.8)$$

For the mass of scalar field excitations (gravexcitons/radions) we obtain  $m^2 = d^2U_{\text{eff}}/d\varphi^2|_{\varphi=0} = (4d_1/(d_1+2))\Lambda_D$ . In Fig. 1, we present the effective potential (2.7) in the case  $d_1 = 3$  and  $\Lambda_D = 10$ . It is worth of noting that usually scalar fields in the present paper are dimensionless<sup>5</sup> and  $U_{\text{eff}}$ ,  $\Lambda_D$ ,  $f_1^2$ ,  $\lambda$  are measured in  $M_{\text{pl}}^2$  units.

Let us turn now to the problem of the external space inflation. As far as the external space corresponds to our Universe, we take metric  $\tilde{g}^{(0)}$  in the spatially flat Friedmann-Robertson-Walker form with scale factor  $a(t)$ . Scalar field  $\varphi$  depends also only on the synchronous/cosmic time  $t$  (in the Einstein frame).

It can be easily seen that for  $\varphi \gg 0$  (more precisely, for  $\varphi > \varphi_{\text{max}} = \sqrt{(d_1+2)/2d_1} \ln 3$ ) the potential (2.7) behaves as

$$U_{\text{eff}}(\varphi) \approx \Lambda_D e^{-\sqrt{q}\varphi}, \quad (2.9)$$

with

$$q := \frac{2d_1}{d_1+2}. \quad (2.10)$$

It is well known (see, e.g., [23–26]) that for such exponential potential scale factor has the following asymptotic form:

$$a(t) \sim t^{2/q}. \quad (2.11)$$

Thus, the Universe undergoes the power-law inflation if  $q < 2$ . Precisely this condition holds for Eq. (2.10) if  $d_1 \geq 1$ .

It can be easily verified that  $\varphi > \varphi_{\text{max}}$  is the only region of the effective potential where inflation takes place. Indeed, in the region  $\varphi < 0$  the leading exponents are too

<sup>5</sup>To restore dimension of scalar fields we should multiply their dimensionless values by  $M_{\text{pl}}/\sqrt{8\pi}$ .

large, i.e., the potential is too steep. The local maximum of the effective potential  $U_{\text{eff}}|_{\text{max}} = (4/27)\Lambda_D$  at  $\varphi_{\text{max}} = \sqrt{(d_1 + 2)/2d_1} \ln 3$  is also too steep for inflation because of the slow-roll parameter  $\eta_{\text{max}} = \frac{1}{U_{\text{eff}}} \frac{d^2 U_{\text{eff}}}{d\varphi^2} |_{\text{max}} = -\frac{3d_1}{d_1+2} \Rightarrow 1 \leq |\eta_{\text{max}}| < 3$  and does not satisfy the inflation condition  $|\eta| < 1$ . Topological inflation is also absent here because the distance between global minimum and local maximum  $\varphi_{\text{max}} = \sqrt{(d_1 + 2)/2d_1} \ln 3 \leq 1.35$  is less than critical value  $\varphi_{\text{cr}} \geq 1.65$  (see [15,27,28]). It is worth of noting that  $\eta_{\text{max}}$  and  $\varphi_{\text{max}}$  depend only on the number of dimensions  $d_1$  of the internal space and do not depend on the height of the local maximum (which is proportional to  $\Lambda_D$ ).

Therefore, we have two distinctive regions in this model. In the first region, at the left of the maximum in the vicinity of the minimum, scalar field undergoes the damped oscillations. These oscillations have the form of massive scalar fields in our Universe (in [3] these excitations were called gravitational excitons and later (see, e.g., [29]) these geometrical moduli oscillations were also named radions). Their lifetime with respect to the decay  $\varphi \rightarrow 2\gamma$  into radiation is [30–32]  $\tau \sim (M_{\text{Pl}}/m)^3 T_{\text{Pl}}$ . For example, we obtain  $\tau \sim 10$  s,  $10^{-2}$  s for  $m \sim 10$  TeV,  $10^2$  TeV, respectively. We remind that in our case  $m^2 = (4d_1/(d_1 + 2))\Lambda_D$ . Therefore, this is the graceful exit region. Here, the internal space scale factor, after the decay of its oscillations into radiation, is stabilized at the present day value, and the effective potential vanishes due to zero minimum. In the second region, at the right of the maximum of the potential, our Universe undergoes the power-low inflation. However, it is impossible to transit from the region of inflation to the graceful exit region because given inflationary solution satisfies the following condition:  $\dot{\varphi} > 0$ . There is also a serious additional problem connected with the obtained inflationary solution. The point is that for the exponential potential of the form (2.9), the spectral index reads as [23,25]<sup>6</sup>:

$$n_s = \frac{2 - 3q}{2 - q}. \quad (2.12)$$

In our case (2.10), it results in  $n_s = 1 - d_1$ . Obviously, for  $d_1 \geq 1$  this value is very far from observable data  $n_s \approx 1$ . Therefore, it is necessary to generalize our linear model.

### III. NONLINEAR QUADRATIC MODEL

As follows from the previous section, we want to generalize the effective potential making it more complicated and with more reach structure. Introduction of an addi-

tional minimal scalar field  $\phi$  is one of possible ways. We can do it “by hand,” inserting the minimal scalar field  $\phi$  with a potential  $U(\phi)$  in the linear action (2.2).<sup>7</sup> Then, effective potential takes the form

$$U_{\text{eff}}(\varphi, \phi) = e^{-\sqrt{(2d_1)/(d_1+2)}\varphi} [U(\phi) + f_1^2 e^{-2\sqrt{(2d_1)/(d_1+2)}\varphi} - \lambda e^{-\sqrt{(2d_1)/(d_1+2)}\varphi}], \quad (3.1)$$

where we put  $\Lambda_D = 0$  in (2.2).

However, it is well known that the scalar field  $\phi$  can naturally originate from the nonlinearity of higher-dimensional models where the Hilbert-Einstein linear Lagrangian  $R$  is replaced by nonlinear one  $f(R)$ . These nonlinear theories are equivalent to the linear ones with a minimal scalar field (which represents additional degree of freedom of the original nonlinear theory). It is not difficult to verify (see, e.g., [13,21]) that nonlinear model

$$S = \frac{1}{2\kappa_D^2} \int_M d^D x \sqrt{|g^{(D)}|} f(\bar{R}) - \frac{1}{2} \int_M d^D x \sqrt{|g^{(D)}|} \frac{1}{d_1!} \times (F^{(1)})^2 - \sum_{k=1}^m \int_{M_0} d^4 x \sqrt{|g^{(0)}(x)|} \tau_{(k)} \quad (3.2)$$

is equivalent to a linear one with conformally related metric

$$g_{ab}^{(D)} = e^{2A\phi/(D-2)} \bar{g}_{ab}^{(D)} \quad (3.3)$$

plus minimal scalar field  $\phi = \ln[df/d\bar{R}]/A$  with a potential of

$$U(\phi) = \frac{1}{2} e^{-B\phi} [\bar{R}(\phi) e^{A\phi} - f(\bar{R}(\phi))], \quad (3.4)$$

where  $A = \sqrt{(D-2)/(D-1)} = \sqrt{(d_1+2)/d_1+3}$  and  $B = D/\sqrt{(D-2)(D-1)} = A(d_1+4)/(d_1+2)$ . After dimensional reduction of this linear model, we obtain an effective  $D_0$ -dimensional action of the form

$$S_{\text{eff}} = \frac{1}{2\kappa_0^2} \int_{M_0} d^{D_0} x \sqrt{|\tilde{g}^{(0)}|} [R[\tilde{g}^{(0)}] - \tilde{g}^{(0)\mu\nu} \partial_\mu \varphi \partial_\nu \varphi - \tilde{g}^{(0)\mu\nu} \partial_\mu \phi \partial_\nu \phi - 2U_{\text{eff}}(\varphi, \phi)], \quad (3.5)$$

with an effective potential exactly of the form of (3.1). It is worth noting that we suppose that matter fields are coupled to the metric  $g^{(D)}$  of the linear theory (see also an analogous approach in [34]).

Let us consider first the *quadratic theory*

$$f(\bar{R}) = \bar{R} + \xi \bar{R}^2 - 2\Lambda_D. \quad (3.6)$$

<sup>6</sup>With respect to conformal time, solution (2.11) reads as  $a(\eta) \sim \eta^{1+\beta}$ , where  $\beta = -(4-q)/(2-q)$ . It was shown in [33] that for such inflationary solution (with  $q < 2$ ) the spectral index of density perturbation is given by  $n_s = 2\beta + 5$  resulting again in (2.12).

<sup>7</sup>If such a scalar field is the only matter field in these models, it is known (see, e.g., [7,13]) that the effective potential can has only negative minimum, i.e., the models are asymptotical anti de Sitter. To uplift this minimum to nonnegative values, it is necessary to add form fields [21].

For this model the scalar field potential (3.4) reads as

$$U(\phi) = \frac{1}{2} e^{-B\phi} \left[ \frac{1}{4\xi} (e^{A\phi} - 1)^2 + 2\Lambda_D \right]. \quad (3.7)$$

It was proven [7] that the internal space is stabilized if the effective potential (3.1) has a minimum with respect to both fields  $\varphi$  and  $\phi$ . It can be easily seen from the form of  $U_{\text{eff}}(\varphi, \phi)$  that the minimum  $\phi_0$  of the potential  $U(\phi)$  coincides with the minimum of  $U_{\text{eff}}(\varphi, \phi)$ :  $dU/d\phi|_{\phi_0} = 0 \rightarrow \partial_\phi U_{\text{eff}}|_{\phi_0} = 0$ . For minimum  $U(\phi_0)$  we obtain [13]

$$U(\phi_0) = \frac{1}{8\xi} x_0^{(-D)/(D-2)} [(x_0 - 1)^2 + 8\xi\Lambda_D], \quad (3.8)$$

where we denote the constant  $x_0 := \exp(A\phi_0) = (A - B + \sqrt{A^2 + (2A - B)B8\xi\Lambda_D}) / (2A - B)$ . It is the global minimum and the only extremum of  $U(\phi)$ . The non-negative minimum of the effective potential  $U_{\text{eff}}$  takes place for positive  $\xi$ ,  $\Lambda_D > 0$ . If  $\xi$ ,  $\Lambda_D > 0$ , the potential  $U(\phi)$  has asymptotic behavior  $U(\phi) \rightarrow +\infty$  for  $\phi \rightarrow \pm\infty$ .

The relations (2.8), where we should make the substitution  $\Lambda_D \rightarrow U(\phi_0)$ , are the necessary and sufficient conditions of the zero minimum of the effective potential  $U_{\text{eff}}(\varphi, \phi)$  at the point  $(\varphi = 0, \phi = \phi_0)$ . Thus, if the parameters of the quadratic models satisfy the conditions  $U(\phi_0) = f_1^2 = \lambda/2$ , we arrive at zero global minimum  $U_{\text{eff}}(0, \phi_0) = 0$ .

It is clear that the profile  $\phi = \phi_0$  of the effective potential  $U_{\text{eff}}$  has a local maximum in the region of  $\varphi > 0$  because  $U_{\text{eff}}(\varphi, \phi = \phi_0) \rightarrow 0$  if  $\varphi \rightarrow +\infty$ . Such a profile has the form shown in Fig. 1. Thus, the effective potential  $U_{\text{eff}}$  has a saddle point  $(\varphi = \varphi_{\text{max}}, \phi = \phi_0)$ , where  $\varphi_{\text{max}} = \sqrt{(d_1 + 2)/2d_1} \ln 3$ . At this point,  $U_{\text{eff}}|_{\text{max}} = (4/27)U(\phi_0)$ . Figure 2 demonstrates the typical contour plot of the effective potential (3.1) with the potential  $U(\phi)$

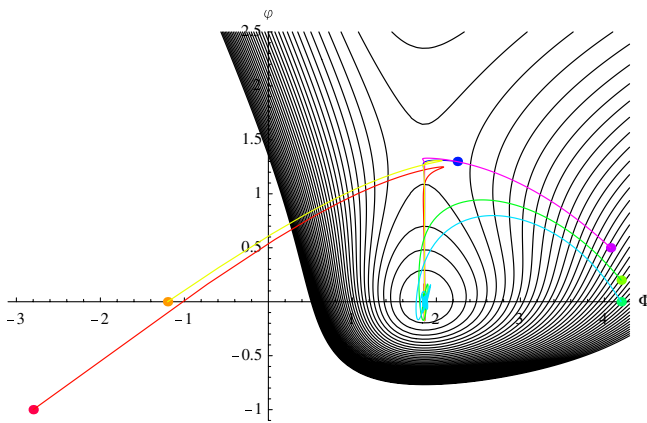


FIG. 2 (color online). Contour plot of the effective potential  $U_{\text{eff}}(\varphi, \phi)$  (3.1) with potential  $U(\phi)$  of the form (3.7) for parameters  $d_1 = 1$ ,  $\xi\Lambda_D = 1$ , and relations  $U(\phi_0) = f_1^2 = \lambda/2$ . This plot clearly shows the global minimum and the saddle. The colored lines describe trajectories for scalar fields starting at different initial conditions.

of the form (3.7) in the vicinity of the global minimum and the saddle point.

Let us discuss now a possibility for the external space inflation in this model. It can be easily realized that for all models of the form (3.1) in the case of local zero minimum at  $(\varphi = 0, \phi_0)$ , the effective potential will also have a saddle point at  $(\varphi = \varphi_{\text{max}}, \phi_0)$  with  $\varphi_{\text{max}} = \sqrt{(d_1 + 2)/2d_1} \ln 3 < \varphi_{\text{cr}} = 1.65$ , and the slow-roll parameter  $|\eta_\varphi|$  in this point cannot be less than 1:  $|\eta_\varphi| = 3d_1/(d_1 + 2) \geq 1$ . Therefore, such saddles are too steep (in the section  $\phi = \phi_0$ ) for the slow-roll and topological inflations. However, as we shall see below, a short period of de Sitter-like inflation is possible if we start not precisely at the saddle point but first move in the vicinity of the saddle along the line  $\varphi \approx \varphi_{\text{max}}$  with subsequent turn into zero minimum along the line  $\phi \approx \phi_0$ . A similar situation happens for trajectories from different regions of the effective potential, which can reach this saddle and spend here a some time (moving along the line  $\varphi \approx \varphi_{\text{max}}$ ).

Let us consider now regions where the following conditions take place:

$$U(\phi) \gg f_1^2 e^{-2\sqrt{(d_1)/(d_1+2)}\varphi}, \quad \lambda e^{-\sqrt{(d_1)/(d_1+2)}\varphi}. \quad (3.9)$$

For the potential (3.7) these regions exist both for negative and positive  $\phi$ . In the case of positive  $\phi$  with  $\exp(A\phi) \gg \max\{1, (8\xi\Lambda_D)^{1/2}\}$  we obtain

$$U_{\text{eff}} \approx \frac{1}{8\xi} e^{-\sqrt{q}\varphi} e^{\sqrt{q_1}\phi}, \quad (3.10)$$

where  $q$  is defined by Eq. (2.10),  $q_1 := (2A - B)^2 = d_1^2 / [(d_1 + 2)(d_1 + 3)]$  and  $q > q_1$ . For potential (3.10) the slow-roll parameters are<sup>8</sup>

$$\epsilon \approx \eta_1 \approx \eta_2 \approx \frac{q}{2} + \frac{q_1}{2} \quad (3.11)$$

and satisfy the slow-roll conditions  $\epsilon, \eta_1, \eta_2 < 1$ . As far as we know, there are no analytic solutions for such a two-scalar-field potential. Anyway, from the form of the potential (3.10) and condition  $q > q_1$  we can get an estimate of  $a \approx t^s$  with  $s \geq 2/q$  (e.g.,  $2/q = 3, 2, 5/3$  for  $d_1 = 1, 2, 3$ , respectively). Thus, in these regions we can get a period of power-law inflation. In spite of a rude character of these estimates, we shall see below that external space scale

<sup>8</sup>In the case of  $n$  scalar fields  $\varphi_i (i = 1, \dots, n)$  with a flat ( $\sigma$  model) target space, the slow-roll parameters for the spatially flat Friedmann Universe read (see, e.g., [7,13]) as  $\epsilon \equiv \frac{2}{H^2} \times \sum_{i=1}^n (\partial_i H)^2 \approx \frac{1}{2} |\partial U|^2 / U^2$ ;  $\eta_i \equiv -\dot{\varphi}_i / (H \dot{\varphi}_i) = 2\partial_i^2 H / H \approx -\epsilon + \sum_{j=1}^n \partial_{ij}^2 U \partial_j U / (U \partial_i U)$ , where  $\partial_i := \partial / \partial \varphi_i$  and  $|\partial U|^2 = \sum_{i=1}^n (\partial_i U)^2$ . In some papers (see, e.g., [35]) a ‘‘cumulative’’ parameter  $\eta \equiv -\sum_{i=1}^n \ddot{\varphi}_i \dot{\varphi}_i / (H |\dot{\varphi}|^2) \approx -\epsilon + \sum_{i,j=1}^n (\partial_{ij}^2 U) \times (\partial_i U)(\partial_j U) / (U |\partial U|^2)$  was introduced, where  $|\dot{\varphi}|^2 = \sum_{i=1}^n \dot{\varphi}_i^2$ . We can easily find that for the potential (3.10) parameter  $\eta$  coincides exactly with parameters  $\eta_1$  and  $\eta_2$ .

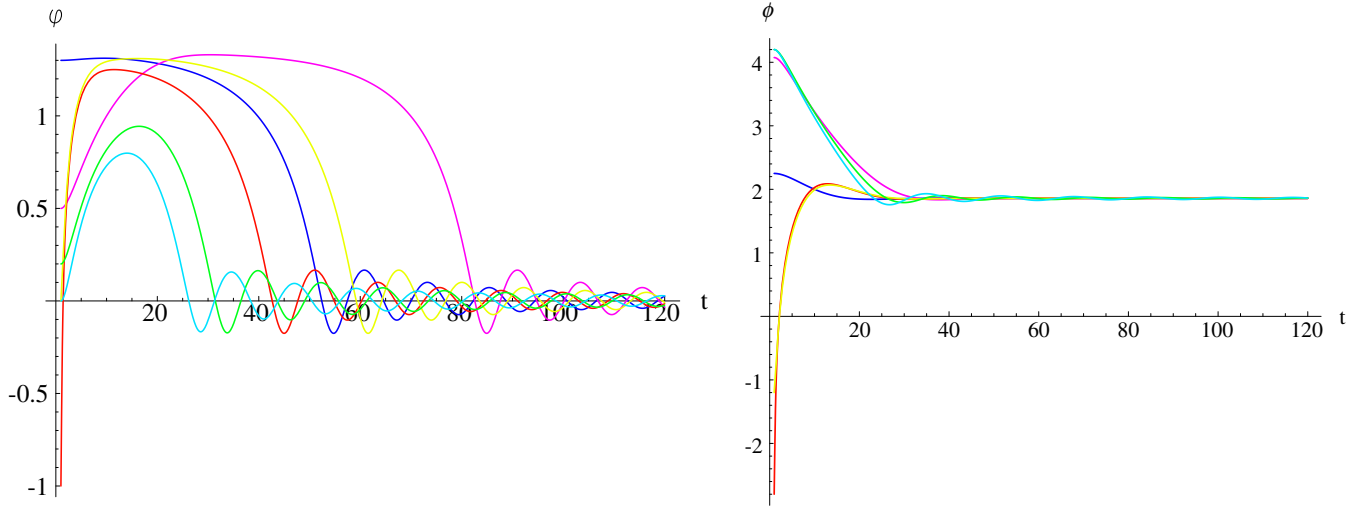


FIG. 3 (color online). Dynamical behavior of scalar fields  $\varphi$  (left panel) and  $\phi$  (right panel) with corresponding initial values denoted by the colored dots in Fig. 2.

factors undergo power-law inflation for trajectories passing through these regions.

Now, we investigate the dynamical behavior of scalar fields and the external space scale factor in more detail. There are no analytic solutions for the considered model. So, we use numerical calculations. To do it, we apply the MATHEMATICA package proposed in [36] adjusting it to our models and notations (see Appendix A).

The colored lines on the contour plot of the effective potential in Fig. 2 describe trajectories for scalar fields  $\varphi$  and  $\phi$  with different initial values (the colored dots). The time evolution of these scalar fields<sup>9</sup> is drawn in Fig. 3. Here, the time  $t$  is measured in the Planck times and classical evolution starts at  $t = 1$ . For given initial conditions, scalar fields approach the global minimum of the effective potential along spiral trajectories.

We plot in Fig. 4 the evolution of the logarithms of the scale factor  $a(t)$  (left panel) and the evolution of the Hubble parameter  $H(t)$  (right panel) and in Fig. 5 the evolution of the parameter of acceleration  $q(t)$ .

Because for the initial condition we use the value  $a(t=1) = 1$  (in the Planck units), then  $\log a(t)$  gives the number of e-folds  $\log a(t) = N(t)$ . Figure 4 shows that for considered trajectories we can reach the maximum of e-folds of the order of 10. Clearly, 10 e-folds is not sufficient to solve the horizon and flatness problems but it can be useful to explain a part of the modern CMB data. For example, the Universe inflates by  $\Delta N \approx 4$  during the period that wavelengths corresponding to the CMB multipoles  $2 \leq l \leq 100$  cross the Hubble radius [37]. However, to have the inflation that is long enough for all modes that contribute to the

<sup>9</sup>We remind that  $\varphi$  describes fluctuations of the internal space scale factor and  $\phi$  reflects the additional degree of freedom of the original nonlinear theory.

CMB to leave the horizon, it is usually supposed that  $\Delta N \geq 15$  [38].

Figure 4 for the evolution of the Hubble parameter (right panel) demonstrates that the red, yellow, dark blue, and pink lines (first four lines from the top) have a plateau  $H \approx \text{const}$ . It means that the scale factor  $a(t)$  has a stage of the de Sitter expansion on these plateaus. Clearly, it happens because these lines reach the vicinity of the effective potential saddle point and spend some time there.

Figure 5 for the acceleration parameter defined in (A6) confirms also the above conclusions. According to Eq. (A8),  $q = 1$  for the de Sitter-like behavior. Indeed, all of these four lines have stages  $q \approx 1$  for the same time intervals when  $H$  has a plateau. Additionally, the magnification of this picture at early times (the right panel of the Fig. 5) shows that pink, green, and blue lines have also a period of time when  $q$  is approximately constant less than one:  $q \approx 0.75$ . In accordance with Eq. (A8), it means that during this time the scale factor  $a(t)$  undergoes the power-law inflation  $a(t) \propto t^s$  with  $s \approx 4$ . This result confirms our rough estimates made above for the trajectories that go through the regions where the effective potential has the form (3.10). After the stages of the inflation, the acceleration parameter starts to oscillate. Averaging  $q$  over a few periods of oscillations, we obtain  $\bar{q} = -0.5$ . Therefore, the scale factor behaves as for the matter dominated Universe  $a(t) \propto t^{2/3}$ . Clearly, it corresponds to the times when the trajectories reach the vicinity of the effective potential global minimum and start to oscillate there. It is worth noting, that there is no need to plot dynamical behavior for the equation of state parameter  $\omega(t)$  because it is linearly connected with  $q$  [see Eq. (A7)], and its behavior can be easily understood from the pictures for  $q(t)$ .

As we have seen above for the considered quadratic model, the maximal number of e-folds is near 10. Can

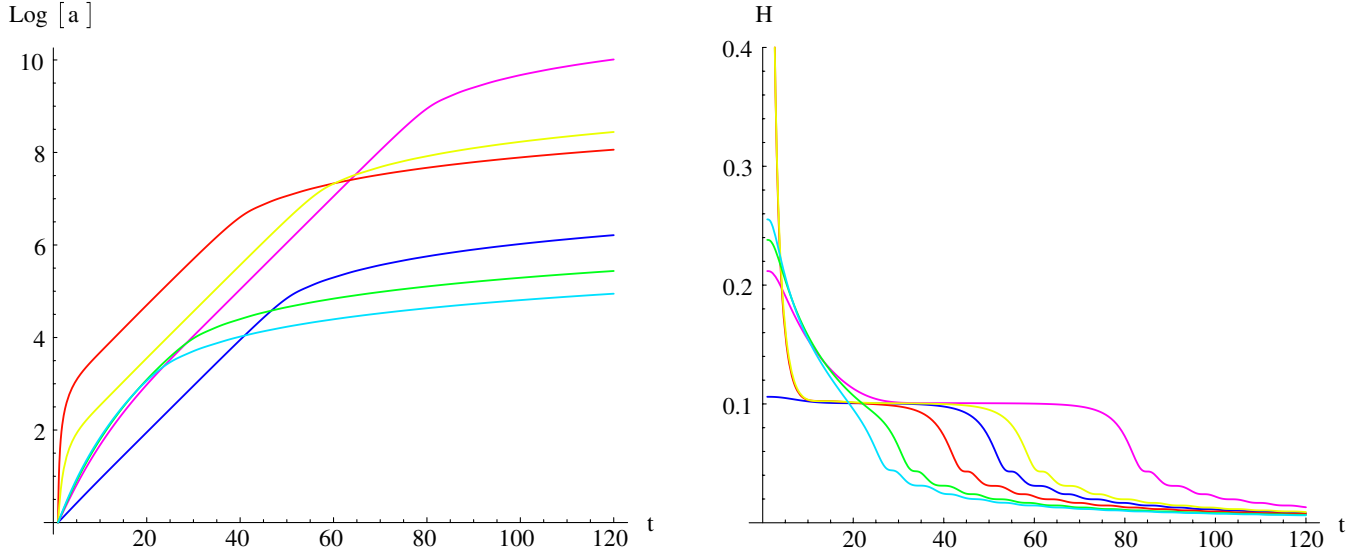


FIG. 4 (color online). The number of e-folds (left panel) and the Hubble parameter (right panel) for the corresponding trajectories.

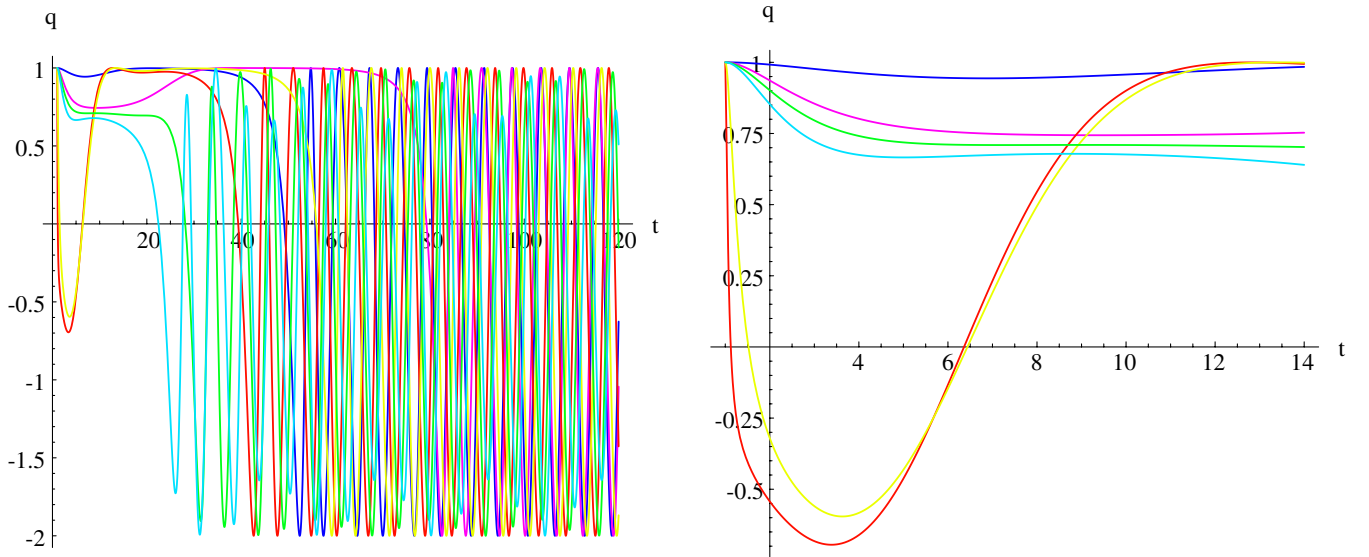


FIG. 5 (color online). The parameter of acceleration (left panel) and its magnification for early times (right panel). There are two different forms of acceleration with  $q \approx 1$  (de Sitter-like inflation) and  $q \approx 0.75$  (power-law inflation with  $s \approx 4$ ), accordingly. The averaging of  $q$  over a few periods of oscillations results in  $\bar{q} = -0.5$ , which corresponds to the matter dominated decelerating Universe.

we increase this number? To answer this question, we shall consider a new model with a higher degree of nonlinearity, i.e., the nonlinear quartic model.

#### IV. NONLINEAR QUARTIC MODEL

In this section we consider the nonlinear quartic model

$$f(\bar{R}) = \bar{R} + \gamma \bar{R}^4 - 2\Lambda_D. \quad (4.1)$$

For this model the scalar field potential (3.4) reads [11] as

$$U(\phi) = \frac{1}{2}e^{-B\phi} \left[ \frac{3}{4}(4\gamma)^{-1/3}(e^{A\phi} - 1)^{4/3} + 2\Lambda_D \right]. \quad (4.2)$$

Here, the scalar curvature  $\bar{R}$  and scalar field  $\phi$  are connected as follows:  $e^{A\phi} \equiv f' = 1 + 4\gamma\bar{R}^3 \Leftrightarrow \bar{R} = [(e^{A\phi} - 1)/4\gamma]^{1/3}$ .

We are looking for a solution that has a non-negative minimum of the effective potential  $U_{\text{eff}}(\varphi, \phi)$  (3.1) where potential  $U(\phi)$  is given by Eq. (4.2). If  $\phi_0$  corresponds to this minimum, then, as we mentioned above (see also [22]),  $U(\phi_0)$ ,  $\lambda$  and  $f_1^2$  should be positive. To get the zero mini-

imum of the effective potential, these positive values should satisfy the relation of the form of (2.8):  $U(\phi_0) = f_1^2 = \lambda/2$ . Additionally, it is important to note that positiveness of  $U(\phi_0)$  results in positive expression for  $\bar{R}(\phi_0) > 0$  [11].

Equation (4.2) shows that the potential  $U(\phi)$  has the following asymptotes for positive  $\gamma$  and  $\Lambda_D$ <sup>10</sup>:  $\phi \rightarrow -\infty \Rightarrow U(\phi) \approx \frac{1}{2} e^{-B\phi} [\frac{3}{4} (4\gamma)^{-1/3} + 2\Lambda_D] \rightarrow +\infty$  and  $\phi \rightarrow +\infty \Rightarrow U(\phi) \approx \frac{3}{8} (4\gamma)^{-1/3} e^{(-B+4A/3)\phi} \rightarrow +0$ . For the latter asymptote we took into account that  $-B + 4A/3 = (D-8)/3\sqrt{(D-2)(D-1)} < 0$  for  $D < 8$ . Obviously, the total number of dimensions  $D = 8$  plays the critical role in quartic nonlinear theories (see [11,14,39]) and investigations for  $D < 8$ ,  $D = 8$ , and  $D > 8$  should be performed separately. To make sure that our paper is not too cumbersome, we consider the case  $D < 8$  (i.e.,  $d_1 = 1, 2, 3$ ), postponing other cases for our following investigations.

It is worth noting that for the considered signs of the parameters, the effective potential  $U_{\text{eff}}(\varphi, \phi)$  (3.1) acquires negative values when  $\phi \rightarrow +\infty$  (and  $U(\phi) \rightarrow 0$ ). For example, if  $U(\phi_0) = f_1^2 = \lambda/2$  (the case of zero minimum of the effective potential), the effective potential  $U_{\text{eff}}(\varphi, \phi \rightarrow \infty) < 0$  for  $0 < e^{-b\varphi} < 2$  and the lowest negative asymptotic value  $U_{\text{eff}}|_{\text{min}} \rightarrow -(16/27)\lambda$  takes place along the line  $e^{-b\varphi} = 4/3$ . Therefore, the zero minimum of  $U_{\text{eff}}$  is local.<sup>11</sup>

As we mentioned above, extremum positions  $\phi_i$  of the potential  $U(\phi)$  coincide with extremum positions of  $U_{\text{eff}}(\varphi, \phi)$ :  $dU/d\phi|_{\phi_i} = 0 \rightarrow \partial_\phi U_{\text{eff}}|_{\phi_i} = 0$ . The condition of extremum for the potential  $U(\phi)$  reads as

$$\frac{dU}{d\phi} = 0 \Rightarrow \bar{R}^4 - \frac{(2+d_1)}{\gamma(4-d_1)} \bar{R} + 2\Lambda_D \frac{(4+d_1)}{\gamma(4-d_1)} = 0. \quad (4.3)$$

For positive  $\gamma$  and  $\Lambda_D$  this equation has two real roots:

$$\bar{R}_{0(1)} = \frac{\Lambda_D}{2} \left( -\sqrt{\frac{2(2+d_1)}{(4-d_1)k\sqrt{M}}} - M + \sqrt{M} \right), \quad (4.4)$$

$$\bar{R}_{0(2)} = \frac{\Lambda_D}{2} \left( \sqrt{\frac{2(2+d_1)}{(4-d_1)k\sqrt{M}}} - M + \sqrt{M} \right), \quad (4.5)$$

where we introduced a dimensionless parameter

$$k := \gamma\Lambda_D^3, \quad (4.6)$$

which is positive for positive  $\gamma$  and  $\Lambda_D$ , and quantities  $M$ ,

<sup>10</sup>Negative values of  $\Lambda_D$  and  $\gamma$  may lead either to negative minima, resulting in an asymptotically anti de Sitter universe, or to infinitely large negative values of  $U_{\text{eff}}$  [11]. In the present paper we want to avoid both of these possibilities. Therefore, we shall consider the case of  $\Lambda_D, \gamma > 0$ . See also Footnote <sup>12</sup>.

<sup>11</sup>It is not difficult to show that the thin shell approximation is valid for the considered model and a tunneling probability from the zero local minimum to this negative  $U_{\text{eff}}$  region is negligible.

$\omega$  read as

$$M \equiv -2^{10/3} \frac{(4+d_1)}{\omega^{1/3}} - \frac{1}{3 \cdot 2^{1/3} k} \frac{\omega^{1/3}}{(4-d_1)}, \quad (4.7)$$

$$\omega \equiv k[-27(4-d_1)(2+d_1)^2 + \sqrt{27^2(4-d_1)^2(2+d_1)^4 - 4 \cdot 24^3 k(16-d_1^2)^3}]. \quad (4.8)$$

It can be easily seen that for  $k > 0$  we get  $\omega < 0$  and  $M \geq 0$ . To have real  $\omega$ , parameter  $k$  should satisfy the following condition:

$$k \leq \frac{27^2(4-d_1)^2(2+d_1)^4}{4 \cdot 24^3(16-d_1^2)^3} \equiv k_0. \quad (4.9)$$

It is not difficult to verify that roots  $\bar{R}_{0(1,2)}$  are real and positive if  $0 < k \leq k_0$ , and they degenerate for  $k \rightarrow k_0$ :  $\bar{R}_{0(1,2)} \rightarrow (\Lambda_D/2)\sqrt{M}$ . In this limit the minimum and maximum of  $U(\phi)$  merge into an inflection point. Now, we should define which of these roots corresponds to a minimum of  $U(\phi)$  and which to a local maximum. The minimum condition

$$\frac{d^2 U(\phi)}{d\phi^2} \Big|_{\phi_0} > 0 \Rightarrow \gamma[(d_1+2) - 4\gamma\bar{R}_0^3(4-d_1)] > 0 \quad (4.10)$$

results in the following inequality<sup>12</sup>:

$$\gamma > 0: (d_1+2) - 4\gamma\bar{R}_0^3(4-d_1) > 0. \quad (4.11)$$

Thus, the root  $\bar{R}_0$ , which corresponds to the minimum of  $U(\phi)$ , should satisfy the following condition:

$$0 < \bar{R}_0 < \left( \frac{d_1+2}{4\gamma(4-d_1)} \right)^{1/3}. \quad (4.12)$$

Numerical analysis shows that  $\bar{R}_{0(1)}$  satisfies these conditions and corresponds to the minimum. For  $\bar{R}_{0(2)}$  we obtain that  $\bar{R}_{0(2)} > \left( \frac{d_1+2}{4\gamma(4-d_1)} \right)^{1/3}$  and corresponds to the local maximum of  $U(\phi)$ . In what follows, we shall use the notations

$$\phi_{\text{min}} = \frac{1}{A} \ln[1 + 4\gamma\bar{R}_{0(1)}^3], \quad (4.13)$$

$$\phi_{\text{max}} = \frac{1}{A} \ln[1 + 4\gamma\bar{R}_{0(2)}^3], \quad (4.14)$$

and  $U(\phi_{\text{min}}) \equiv U_{\text{min}}$ ,  $U(\phi_{\text{max}}) \equiv U_{\text{max}}$ . We should note that  $\phi_{\text{min}}$ ,  $\phi_{\text{max}}$ , and the ratio  $U_{\text{max}}/U_{\text{min}}$  depend on the combination  $k$  (4.6) rather than on  $\gamma$  and  $\Lambda_D$  taken separately.

<sup>12</sup>As we have already mentioned above, the condition  $U(\phi_0) > 0$  leads to the inequality  $\bar{R}(\phi_0) > 0$  [11]. Taking into account the condition  $d_1 < 4$ , we clearly see that inequality  $(d_1+2) + 4|\gamma|\bar{R}_0^3(4-d_1) < 0$  for  $\gamma < 0$  cannot be realized. This is an additional argument in favor of positive sign of  $\gamma$ .

TABLE I. The number of extrema of the effective potential  $U_{\text{eff}}$  depending on the relation between parameters.

$0 < \alpha < \alpha_1$	$\alpha = \alpha_1$	$\alpha_1 < \alpha < \alpha_2$	$\alpha = \alpha_2$	$\alpha > \alpha_2$
No extrema	One extremum (point of inflection on the line $\phi = \phi_{\min}$ )	Two extrema (one minimum and one saddle on the line $\phi = \phi_{\min}$ )	Three extrema (minimum and saddle on the line $\phi = \phi_{\min}$ inflection on the line $\phi = \phi_{\max}$ )	Four extrema (minimum and saddle on the line $\phi = \phi_{\min}$ maximum and saddle on the line $\phi = \phi_{\max}$ )

Obviously, because potential  $U(\phi)$  has two extrema at  $\phi_{\min}$  and  $\phi_{\max}$ , the effective potential  $U_{\text{eff}}(\varphi, \phi)$  may have points of extrema only on the lines  $\phi = \phi_{\min}$  and  $\phi = \phi_{\max}$ , where  $\partial U_{\text{eff}}/\partial \phi|_{\phi_{\min}, \phi_{\max}} = 0$ . To find the extrema of  $U_{\text{eff}}$ , it is necessary to consider the second extremum condition  $\partial U_{\text{eff}}/\partial \varphi = 0$  on each line separately:

$$\frac{\partial U_{\text{eff}}}{\partial \varphi} = 0 \Rightarrow \begin{cases} -U_{\min} - 3f_1^2 \chi_1^2 + 2\lambda \chi_1 = 0, \\ -U_{\max} - 3f_1^2 \chi_2^2 + 2\lambda \chi_2 = 0, \end{cases} \quad (4.15)$$

where  $\chi_1 \equiv \exp(-\sqrt{2d_1/(d_1+2)}\varphi_1) > 0$  and  $\chi_2 \equiv \exp(-\sqrt{2d_1/(d_1+2)}\varphi_2) > 0$ ;  $\varphi_1$  and  $\varphi_2$  denote positions of extrema on the lines  $\phi = \phi_{\min}$  and  $\phi = \phi_{\max}$ , respectively. These equations have the solutions

$$\chi_{1(\pm)} = \alpha \pm \sqrt{\alpha^2 - \beta}, \quad \alpha \geq \sqrt{\beta} \equiv \alpha_1; \quad (4.16)$$

$$\begin{aligned} \chi_{2(\pm)} &= \alpha \pm \sqrt{\alpha^2 - \beta \frac{U_{\max}}{U_{\min}}}, \\ \alpha &\geq \sqrt{\beta \frac{U_{\max}}{U_{\min}}} \equiv \alpha_2 > \alpha_1; \end{aligned} \quad (4.17)$$

where we have introduced the notations  $\alpha \equiv \lambda/(3f_1^2)$  and  $\beta \equiv U_{\min}/(3f_1^2)$ . These equations show that there are five different possibilities, which are listed in the Table I.

To clarify which of the solutions (4.16) and (4.17) correspond to minima of the effective potential (with respect to  $\varphi$ ) we should consider the minimum condition

$$\left. \frac{\partial^2 U_{\text{eff}}}{\partial^2 \varphi} \right|_{\min} > 0 \Rightarrow U_{\text{extr}} + \chi^2 9f_1^2 - 4\lambda \chi > 0, \quad (4.18)$$

where  $U_{\text{extr}}$  is either  $U_{\min}$  or  $U_{\max}$ , and  $\chi$  denotes either  $\chi_1$  or  $\chi_2$ . Taking into account relations (4.15), we obtain

$$\chi^2 3f_1^2 - \chi \lambda > 0 \Rightarrow \chi > \frac{\lambda}{3f_1^2} = \alpha. \quad (4.19)$$

Thus, roots  $\chi_{1,2(+)}$  define the positions of local minima of the effective potential with respect to the variable  $\varphi$ , and  $\chi_{1,2(-)}$  correspond to local maxima (in the direction of  $\varphi$ ).

Now, we fix the minimum  $\chi_{1(+)}$  at the point  $\varphi = 0$ . It means that in this local minimum the internal space scale factor is stabilized at the present day value. In this case,

$$\chi_{1(+)}|_{\varphi=0} = 1 = \alpha + \sqrt{\alpha^2 - \beta} \Rightarrow \alpha = \frac{1 + \beta}{2}. \quad (4.20)$$

Obviously, we can do it only if<sup>13</sup>  $\alpha < 1 \Rightarrow \beta \in [0, 1)$ . For  $\chi_{1(-)}$  we get  $\chi_{1(-)} = \beta$ .

Additionally, the local minimum of the effective potential at the point ( $\varphi = 0, \phi = \phi_{\min}$ ) should play the role of the non-negative four-dimensional effective cosmological constant. Thus, we arrive at the following condition:

$$\begin{aligned} \Lambda_{\text{eff}} \equiv U_{\text{eff}}(\varphi = 0, \phi = \phi_{\min}) &= -\lambda + U_{\min} + f_1^2 \geq 0 \\ \Rightarrow -\alpha + \beta + \frac{1}{3} &\geq 0. \end{aligned} \quad (4.21)$$

From the latter inequality and Eq. (4.20) we get  $\beta \in [1/3, 1)$ . It can be easily seen that  $\beta = 1/3$  (and, correspondingly,  $\alpha = 2/3$ ) results in  $\Lambda_{\text{eff}} = 0$  and we obtain the above mentioned relations  $U_{\min} = f_1^2 = \lambda/2$ . In general, it is possible to demand that  $\Lambda_{\text{eff}}$  coincides with the present day dark energy value  $10^{-57} \text{ cm}^{-2}$ . However, it leads to a very flat local minimum, which means the decompactification of the internal space [22]. In what follows, we shall mainly consider the case of zero  $\Lambda_{\text{eff}}$ , although all obtained results are trivially generalized to  $\Lambda_{\text{eff}} = 10^{-57} \text{ cm}^{-2}$ .

Summarizing our results, in the most interesting case of  $\alpha > \alpha_2$  the effective potential has four extrema: local minimum at  $(\varphi|_{\chi_{1(+)}}, \phi_{\min})$ , local maximum at  $(\varphi|_{\chi_{2(-)}}, \phi_{\max})$  and two saddle-points at  $(\varphi|_{\chi_{1(-)}}, \phi_{\min})$ , and  $(\varphi|_{\chi_{2(+)}}, \phi_{\max})$  (see Fig. 7).

We pay particular attention to the case of zero local minimum  $U_{\text{eff}}(\varphi|_{\chi_{1(+)}}, \phi_{\min}) = 0$ , where  $\beta = 1/3 \Rightarrow \alpha = (1 + \beta)/2 = 2/3$ . To satisfy the four-extremum condition  $\alpha > \alpha_2$ , we should demand

$$\frac{U_{\max}}{U_{\min}} < \frac{4}{3}. \quad (4.22)$$

The fraction  $U_{\max}/U_{\min}$  is the function of  $k$  and depends parametrically only on the internal space dimension  $d_1$ . Inequality (4.22) provides the lower bound on  $k$  and numerical analysis (see Fig. 6) gives  $\tilde{k}(d_1 = 1) \approx 0.000625$ ;  $\tilde{k}(d_1 = 2) \approx 0.00207$ ;  $\tilde{k}(d_1 = 3) \approx 0.0035$ . Therefore, effective potentials with zero local minimum will have four extrema if  $k \in (\tilde{k}, k_0)$  [where  $k_0$  is defined by Eq. (4.9)]. The limit  $k \rightarrow \tilde{k}$  results in merging  $\chi_{2(-)} \leftrightarrow \chi_{2(+)}$ , and the

<sup>13</sup>Particular value  $\alpha = 1$  corresponds to the case  $\alpha = \alpha_1 = 1$ , where the only extremum is the inflection point with  $\chi_{1(-)} = \chi_{1(+)} = \alpha = 1$ . Here,  $\lambda = U_{\min} = 3f_1^2$  and  $U_{\text{eff}}(\varphi = 0, \phi = \phi_{\min}) = -\lambda + U_{\min} + f_1^2 > 0$ .

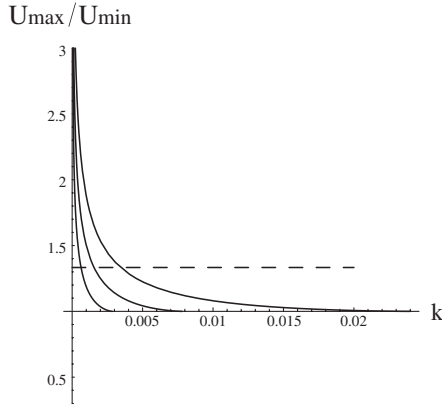


FIG. 6. The form of  $U_{\max}/U_{\min}$  as a function of  $k \in (0, k_0]$  for  $d_1 = 1, 2, 3$  from left to right, respectively. The dashed line corresponds to  $U_{\max}/U_{\min} = 4/3$ .

limit  $k \rightarrow k_0$  results in merging  $\chi_{1(-)} \leftrightarrow \chi_{2(-)}$  and  $\chi_{1(+)} \leftrightarrow \chi_{2(+)}$ . Such merging results in the transformation of corresponding extrema into inflection points. For example, from Fig. 6, it follows that  $U_{\max}/U_{\min} \rightarrow 1$  for  $k \rightarrow k_0$ .

The typical contour plot of the effective potential with four extrema in the case of zero local minimum is drawn in Fig. 7. Here, for  $d_1 = 3$  we take  $k = 0.004 \in (\tilde{k}, k_0)$ , which gives  $\alpha_2 \approx 0.655$ . Thus,  $\alpha = 2/3 \approx 0.666 > \alpha_2$ .

Let us investigate now a possibility of inflation for the considered potential. First of all, taking into account the comments in the previous section [see the paragraph before Eq. (3.9)], it is clear that topological inflation in the saddle point  $\chi_{1(-)}$  as well as the slow rolling from there in the direction of the local minimum  $\chi_{1(+)}$  are absent. It is not difficult to verify that the generalized power-law inflation

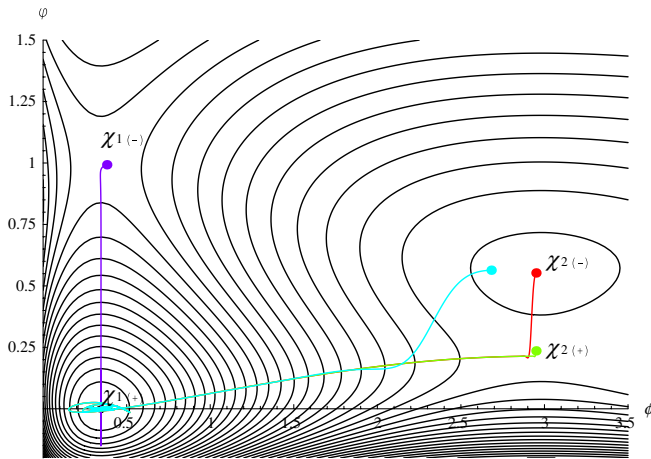


FIG. 7 (color online). Contour plot of the effective potential  $U_{\text{eff}}(\varphi, \phi)$  (3.1) with potential  $U(\phi)$  of the form (4.2) for parameters  $\beta = 1/3$ ,  $d_1 = 3$ , and  $k = 0.004$ . This plot shows the local zero minimum, local maximum, and two saddles. The colored lines describe trajectories for scalar fields starting at different initial conditions.

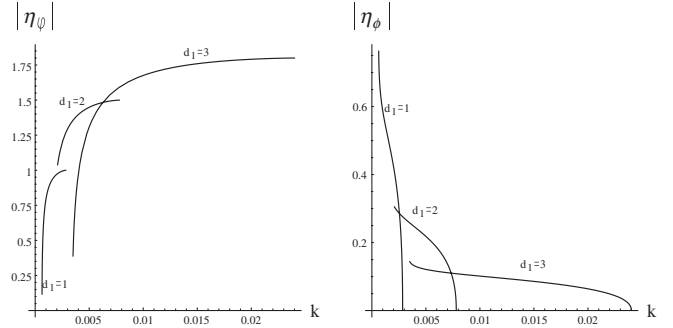


FIG. 8. Graphs of  $|\eta_\varphi|$  (left panel) and  $|\eta_\phi|$  (right panel) as functions of  $k \in (\tilde{k}, k_0)$  for local maximum  $\chi_{2(-)}$  and parameters  $\beta = 1/3$  and  $d_1 = 1, 2, 3$ .

discussed in the case of the nonlinear quadratic model is also absent here. Indeed, from Eqs. (3.1) and (4.2) it follows that the nonlinear potential  $U(\phi)$  can play the leading role in the region  $\phi \rightarrow -\infty$  (because  $U(\phi) \rightarrow 0$  for  $\phi \rightarrow +\infty$ ). In this region,  $U_{\text{eff}} \propto \exp(-\sqrt{q}\varphi) \times \exp(-\sqrt{q_2}\phi)$ , where  $q = 2d_1/(d_1 + 2)$  and  $q_2 = B^2 = (d_1 + 4)^2/[(d_1 + 2)(d_1 + 3)]$ . For these values of  $q$  and  $q_2$  the slow-roll conditions are not satisfied:  $\epsilon \approx \eta_1 \approx \eta_2 \approx q/2 + q_2/2 > 1$ . However, there are two promising regions where the stage of inflation with subsequent stable compactification of the internal space may take place. We mean the local maximum  $\chi_{2(-)}$  and the saddle  $\chi_{2(+)}$  (see Fig. 7). Let us estimate the slow-roll parameters for these regions.

We consider first the local maximum  $\chi_{2(-)}$ . It is obvious that the parameter  $\epsilon$  is equal to zero here. Additionally, from the form of the effective potential (3.1) it is clear that the mixed second derivatives are also absent in extremum points. Thus, the slow-roll parameters  $\eta_1$  and  $\eta_2$ , defined in Footnote 8, coincide exactly with  $\eta_\varphi$  and  $\eta_\phi$ . In Fig. 8 we present typical form of these parameters as functions of  $k \in (\tilde{k}, k_0)$  in the case  $\beta = 1/3$  and  $d_1 = 1, 2, 3$ . These plots show that, for considered parameters, the slow-roll inflation in this region is possible for  $d_1 = 1, 3$ .

The vicinity of the saddle point  $\chi_{2(+)}$  is another promising region. Obviously, if we start from this point, a test particle will roll mainly along direction of  $\phi$ . That is why it makes sense to draw only  $|\eta_\phi|$ . In Fig. 9, we plot a typical form of  $|\eta_\phi|$  in the case of  $\beta = 1/3$  and  $d_1 = 1, 2, 3$ . The left panel represents general behavior for the whole range of  $k \in (\tilde{k}, k_0)$ , and the right panel shows detailed behavior in the most interesting region of small  $k$ . It shows that  $d_1 = 3$  is the most promising case in this region.

Now, we investigate numerically the dynamical behavior of scalar fields and the external space scale factor for trajectories that start from the regions  $\chi_{1(-)}$ ,  $\chi_{2(-)}$  and  $\chi_{2(+)}$ . All numerical calculations are performed for  $\beta = 1/3$ ,  $d_1 = 3$ , and  $k = 0.004$ . The colored lines on the contour plot of the effective potential in Fig. 7 describe trajectories for scalar fields  $\varphi$  and  $\phi$  with different initial

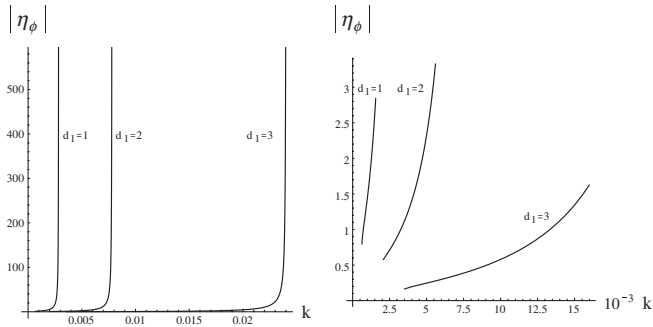


FIG. 9. Graphs of  $|\eta_\phi|$  as functions of  $k$  for saddle point  $\chi_{2(+)}$  and parameters  $\beta = 1/3$  and  $d_1 = 1, 2, 3$ . The left panel demonstrates the whole region of variable  $k \in (\tilde{k}, k_0)$ , and the right panel shows detailed behavior for small  $k$ .

values (the colored dots) in the vicinity of these extrema points. The time evolution of these scalar fields is drawn in Fig. 10. For given initial conditions, scalar fields approach the local minimum  $\chi_{1(+)}$  of the effective potential along the spiral trajectories.

We plot in Fig. 11 the evolution of the logarithm of the scale factor  $a(t)$  (left panel), which gives directly the number of e-folds and the evolution of the Hubble parameter  $H(t)$  (right panel) and in Fig. 12 the evolution of the parameter of acceleration  $q(t)$ .

Figure 11 shows that for considered trajectories we can reach the maximum of e-folds of the order of 22, which is long enough for all modes that contribute to the CMB to leave the horizon.

The Fig. 11 for the evolution of the Hubble parameter (right panel) demonstrates that all lines have plateaus  $H \approx \text{const}$ . However, the red, yellow, and blue lines, which pass in the vicinity of the saddle  $\chi_{2(+)}$ , have bigger value of the Hubble parameter with respect to the dark blue line, which

starts from the  $\chi_{1(-)}$  region. Therefore, the scale factor  $a(t)$  has stages of the de Sitter-like expansion corresponding to these plateaus, which last approximately from 100 (dark blue line) up to 800 (red line) Planck times.

Figure 12 for the acceleration parameter also confirms the above conclusions. All four lines have stages  $q \approx 1$  for the same time intervals when  $H$  has plateaus. After the stages of inflation, the acceleration parameter starts to oscillate. Averaging  $q$  over a few periods of oscillations, we obtain  $\bar{q} = -0.5$ . Therefore, the scale factor behaves as for the matter dominated Universe  $a(t) \propto t^{2/3}$ . Clearly, it corresponds to the times when the trajectories reach the vicinity of the effective potential local minimum  $\chi_{1(+)}$  and start to oscillate there.

Let us investigate now a possibility for topological inflation [16,40] if the scalar fields  $\varphi, \phi$  stay in the vicinity of the saddle point  $\chi_{2(+)}$ . As we mentioned in Sec. II, topological inflation in the case of the double-well potential takes place if the distance between a minimum and local maximum is bigger than  $\Delta\phi_{\text{cr}} = 1.65$ . In this case, the domain wall is thick enough in comparison with the Hubble radius. The critical ratio of the characteristic thickness of the wall to the horizon scale in local maximum is  $r_w H \approx |U/3\partial U_{\phi\phi}|^{1/2} \approx 0.48$  [27], and for topological inflation it is necessary to exceed this critical value. Therefore, we should examine the saddle  $\chi_{2(+)}$  from the point of these criteria.

In Fig. 13 (left panel), we draw the difference  $\Delta\phi = \phi_{\text{max}} - \phi_{\text{min}}$  for the profile  $\varphi = \varphi|_{\chi_{2(+)}}$  as a functions of  $k \in (\tilde{k}, k_0)$  in the case of  $\beta = 1/3$  for dimensions  $d_1 = 1, 2, 3$ . This picture shows that this difference can exceed the critical value if the number of the internal dimensions is  $d_1 = 2$  and  $d_1 = 3$ . The right panel of Fig. 13 confirms this conclusion. Here, we consider the case of  $\beta = 1/3$ ,  $k = 0.004$ , and  $d_1 = 3$ . For chosen values of the parameters,

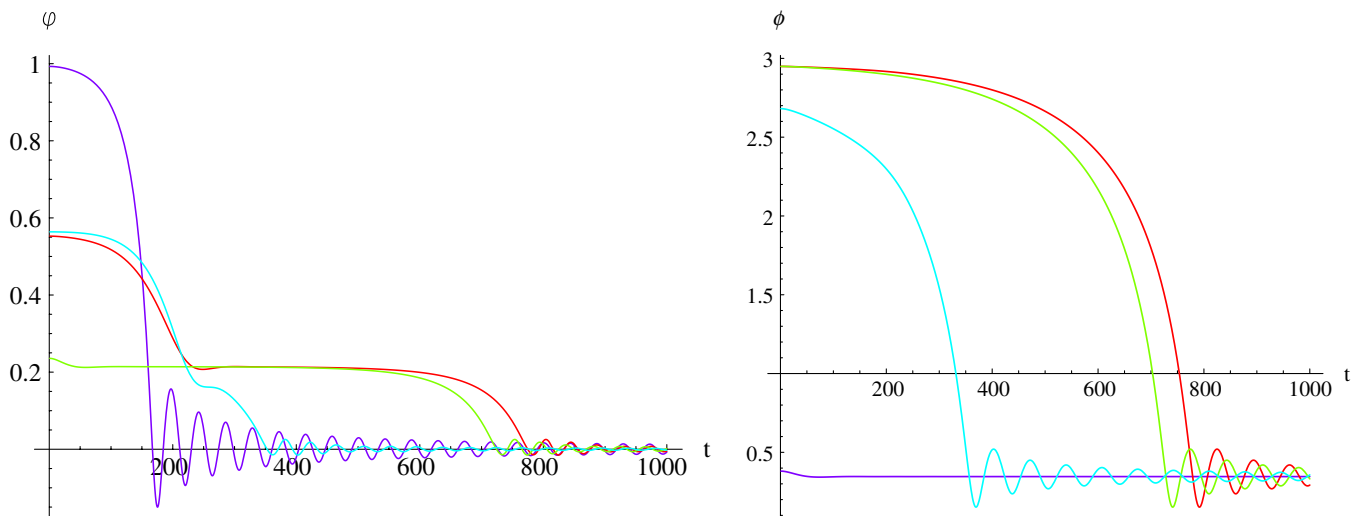


FIG. 10 (color online). Dynamical behavior of scalar fields  $\varphi$  (left panel) and  $\phi$  (right panel) with corresponding initial values denoted by the colored dots in Fig. 7.

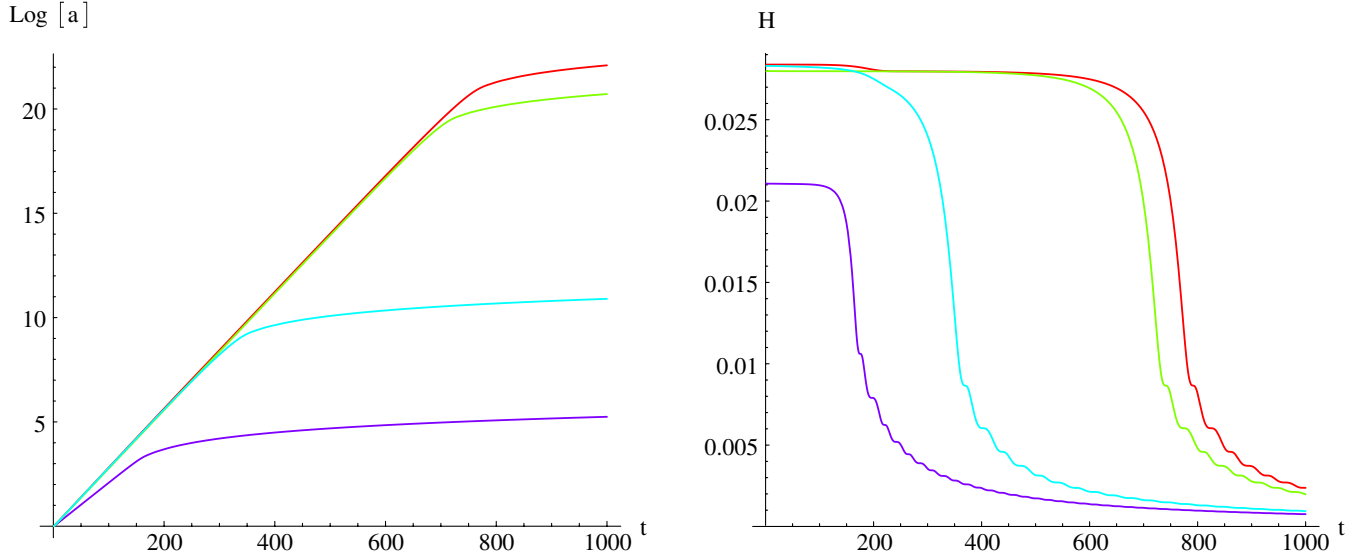


FIG. 11 (color online). The number of e-folds (left panel) and the Hubble parameter (right panel) for the corresponding trajectories.

$\Delta\phi = 2.63$ , which is considerably bigger than the critical value 1.65 and the ratio of the thickness of the wall to the horizon scale is 1.30, which again is bigger than the critical value 0.48. Therefore, topological inflation can happen for the considered model. Moreover, due to quantum fluctuations of scalar fields, the inflating domain wall will have fractal structure: it will contain many other inflating domain walls, and each of these domain walls again will contain new inflating domain walls and so on [16]. Thus, from this point, such a topological inflation is the eternal one.

To conclude this section, we want to draw the attention to one interesting feature of the given model. From the above consideration, it follows that in the case of the zero

minimum of the effective potential the positions of extrema are fully determined by the parameters  $k$  and  $d_1$  and for fixed  $k$ , and  $d_1$  do not depend on the choice of  $\Lambda_D$ . The same takes place for the slow-roll parameters. On the other hand, if we keep  $k$  and  $d_1$ , the height of the effective potential is defined by  $\Lambda_D$  (see Appendix B). Therefore, we can change the height of extrema with the help of  $\Lambda_D$  but preserve the conditions of inflation for given  $k$  and  $d_1$ .

However, the dynamical characteristics of the model (drawn in Figs. 10–12) depend on variations of  $\Lambda_D$  by the self-similar manner. It means that the change of height of the effective potential via transformation  $\Lambda_D \rightarrow c\Lambda_D$  ( $c$  is a constant) with fixed  $k$  and  $d_1$  results in the rescaling of Figs. 10–12 in  $1/\sqrt{c}$  times along the time axis.

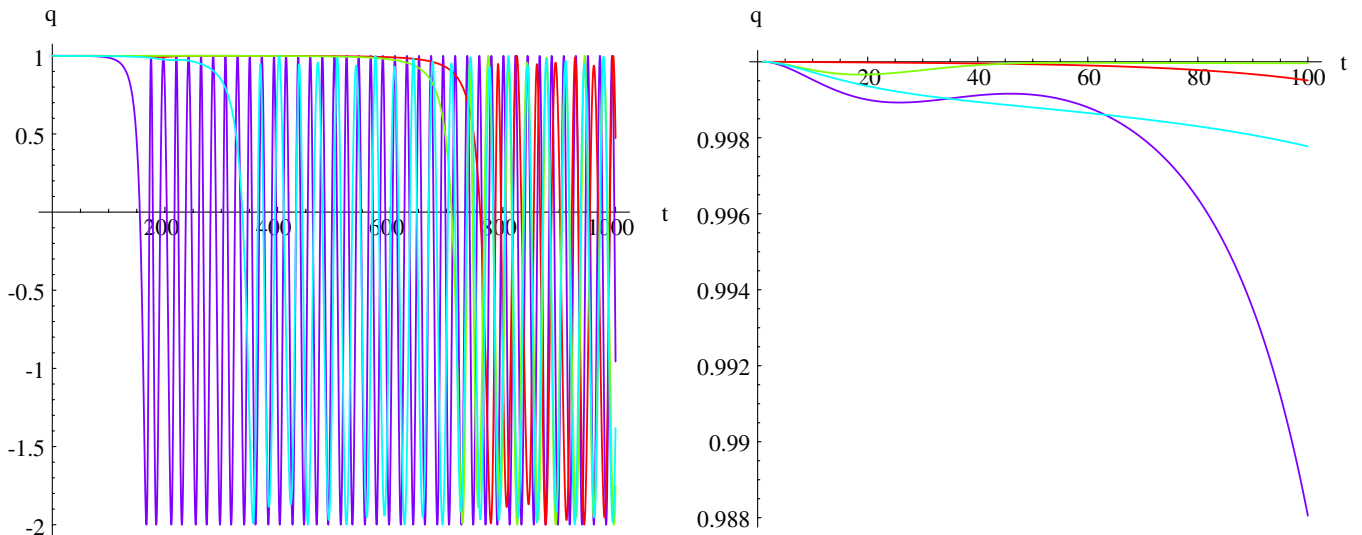


FIG. 12 (color online). The parameter of acceleration (left panel) and its magnification for early times (right panel).

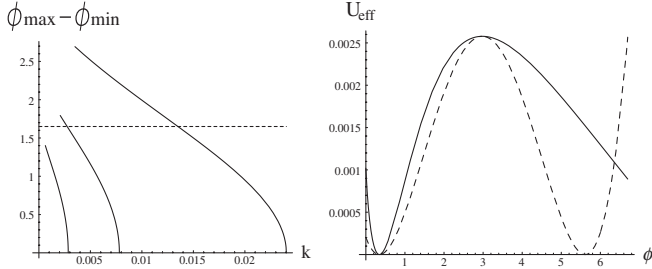


FIG. 13. The left panel demonstrates the difference of  $\phi_{\max} - \phi_{\min}$  (for the profile  $\varphi = \varphi|_{\chi_{2(+)}}$ ) as a functions of  $k \in (\tilde{k}, k_0)$  for parameters  $\beta = 1/3$ , and  $d_1 = 1, 2, 3$  (from left to right, respectively). The dashed line corresponds to  $\phi_{\max} - \phi_{\min} = 1.65$ . The right panel shows the comparison of the potential  $U_{\text{eff}}(\varphi|_{\chi_{2(+)}, \phi})$  with a double-well potential for parameters  $\beta = 1/3$ ,  $k = 0.004$ , and  $d_1 = 3$ .

## V. SUMMARY AND DISCUSSION

In our paper we investigated the possibility of inflation in multidimensional cosmological models. We paid particular attention to nonlinear (in scalar curvature) models with quadratic  $R^2$  and quartic  $R^4$  Lagrangians. These models contain two scalar fields. One of them corresponds to the scale factor of the internal space, and the other one is related to the  $R$  nonlinearity of the original models. The effective four-dimensional potentials in these models are completely determined by the geometry and the matter content of the models. The geometry is defined by the direct product of the Ricci-flat external and internal spaces. As a matter source, we include a monopole form field, a D-dimensional bare cosmological constant and the tensions of the branes located at the fixed points. The exact form of the effective potentials depends on the relation between various model parameters and can take a rather complicated form with a number of extrema points.

First of all, we found the parameter range that insures the existence of zero minima of the effective potentials. These minima provide a sufficient condition for a stabilization of the internal space and, consequently, to avoid the problem of varying fundamental constants. Zero minima correspond to a zero effective four-dimensional cosmological constant. In general, we can also consider a positive effective cosmological constant, which could be identified with the presently observed dark energy. However, usually this requires an extreme fine-tuning of the parameters of the models.

Then, for corresponding effective potentials, we investigated the possibility for inflation of the external space. We have shown that for some initial conditions in the quadratic and quartic models we can achieve up to 10 and 22 e-folds, respectively. An additional bonus of the considered model is that the  $R^4$  model can provide conditions for eternal topological inflation.

Obviously, 10 and 22 e-folds are not sufficient to solve the homogeneity and isotropy problem, but they are cer-

tainly big enough to explain the recent CMB data. To have an inflation that is long enough for modes that contribute to the CMB, it is usually supposed that  $\Delta N \geq 15$  [38]. Moreover, 22 e-folds is a rather big number to encourage investigations of nonlinear multidimensional models and to search for theories where this number will approach 50–60. We have seen that increasing the nonlinearity (from quadratic to quartic one) results in increasing  $\Delta N$  by a factor of 2. So, there is justified hope that more complicated nonlinear models can provide the necessary 50–60 e-folds. Besides, this number is reduced in models where a long matter dominated (MD) stage that follows inflation can subsequently decay into radiation [41,42]. Precisely this scenario takes place for our models. We have shown for quadratic and quartic nonlinear models, that the MD stage with an external scale factor of  $a \sim t^{2/3}$  takes place after the stage of inflation. This happens when the scalar fields start to oscillate near the position of a zero minimum of the effective potential. However, the scalar fields are not stable. For example, the scalar field  $\varphi$  decays into two photons  $\varphi \rightarrow 2\gamma$  with a decay rate  $\Gamma \sim m_\varphi^3/M_{\text{Pl}}^2$  [30]. Thus, the lifetime is  $\tau_{\text{decay}} \sim (M_{\text{Pl}}/m_\varphi)^3 t_{\text{Pl}}$ . The reheating temperature is given by the expression  $T_{\text{RH}} \sim (m_\varphi^3/M_{\text{Pl}})^{1/2}$ . Therefore, to get  $T_{\text{RH}} \geq 1$  MeV as necessary for nucleosynthesis, we should take  $m_\varphi \geq 10$  TeV. In Ref. [42], it was shown that for such a scenario with an intermediate MD stage, the necessary number of e-folds is reduced according to the formula

$$\Delta N = -\frac{1}{6} \ln\left(\frac{45}{2} g_*^{-3/2} \frac{m_\varphi^2}{\Gamma M_{\text{Pl}}}\right) = -\frac{1}{6} \ln\left(\frac{45}{2} g_*^{-3/2} \frac{M_{\text{Pl}}}{m_\varphi}\right), \quad (5.1)$$

where  $g_*$  counts the effective number of relativistic degrees of freedom and where we took into account that decaying particles are scalars. This expression weakly depends on  $g_*$ . For example, if  $m_\varphi \sim 10$  TeV, we obtain  $-6.27 \leq \Delta N \leq -5.11$  for  $1 \leq g_* \leq 10^2$ . Thus,  $\Delta N \approx -6$ . Therefore, we believe that the number of e-folds is not a big problem for multidimensional nonlinear models. The main problem consists in the spectral index. For example, in the case of the  $R^4$  model we get  $n_s \approx 1 + 2\eta|_{\chi_{2(+)}} \approx 0.61$ , which is less than the presently observed  $n_s \approx 1$ . A possible solution of this problem may consist in a more general form of the nonlinearity  $f(R)$ . It was observed in [15] that considering quadratic and quartic nonlinearities simultaneously we can flatten the effective potential and increase  $n_s$ . We postpone this problem to separate investigations.

## ACKNOWLEDGMENTS

A. Zh. acknowledges the hospitality of the Theory Division of CERN where this work has been started. A. Zh. would like to thank the Abdus Salam International Center for Theoretical Physics (ICTP) for their kind hos-

pitality during the final stage of this work. This work was supported in part by the ‘‘Cosmomicrophysics’’ programme of the Physics and Astronomy Division of the National Academy of Sciences of Ukraine.

## APPENDIX A: FRIEDMANN EQUATIONS FOR THE MULTICOMPONENT SCALAR FIELD MODEL

We consider  $n$  scalar fields minimally coupled to gravity in four dimensions. The effective action of this model reads as

$$S = \frac{1}{16\pi G} \int d^4x \sqrt{|\tilde{g}^{(0)}|} (R[\tilde{g}^{(0)}] - G_{ij} \tilde{g}^{(0)\mu\nu} \partial_\mu \varphi^i \partial_\nu \varphi^j - 2U(\varphi^1, \varphi^2, \dots)), \quad (\text{A1})$$

where the kinetic term is usually taken in the canonical form  $G_{ij} = \text{diag}(1, 1, \dots)$  (flat  $\sigma$  model). Such multicomponent scalar fields originate naturally in multidimensional cosmological models (with linear or nonlinear gravitational actions) [3,7,13]. We use the usual conventions  $c = \hbar = 1$ , i.e.,  $L_{\text{Pl}} = t_{\text{Pl}} = 1/M_{\text{Pl}}$  and  $8\pi G = 8\pi/M_{\text{Pl}}^2$ . Here, scalar fields are dimensionless, and potential  $U$  has dimension  $[U] = \text{length}^{-2}$ .

Because we want to investigate the dynamical behavior of our Universe in the presence of scalar fields, we suppose that scalar fields are homogeneous:  $\varphi^i = \varphi^i(t)$  and the four-dimensional metric is spatially flat Friedmann-Robertson-Walker one  $\tilde{g}^{(0)} = -dt \otimes dt + a^2(t) d\vec{x} \otimes d\vec{x}$ .

For energy density and pressure we easily get

$$\rho = \frac{1}{8\pi G} \left( \frac{1}{2} G_{ij} \dot{\varphi}^i \dot{\varphi}^j + U \right), \quad (\text{A2})$$

$$P = \frac{1}{8\pi G} \left( \frac{1}{2} G_{ij} \dot{\varphi}^i \dot{\varphi}^j - U \right);$$

$$\Rightarrow \begin{cases} \frac{1}{2} G_{ij} \dot{\varphi}^i \dot{\varphi}^j = 4\pi G(\rho + P), \\ U = 4\pi G(\rho - P). \end{cases} \quad (\text{A3})$$

The Friedmann equations for considered model are

$$3\left(\frac{\dot{a}}{a}\right)^2 \equiv 3H^2 = 8\pi G\rho = \frac{1}{2} G_{ij} \dot{\varphi}^i \dot{\varphi}^j + U, \quad (\text{A4})$$

and

$$\dot{H} = -4\pi G(\rho + P) = -\frac{1}{2} G_{ij} \dot{\varphi}^i \dot{\varphi}^j. \quad (\text{A5})$$

From these two equations, we obtain the following expression for the acceleration parameter:

$$q \equiv \frac{\ddot{a}}{H^2 a} = 1 - \frac{4\pi G}{H^2} (\rho + P) = -\frac{8\pi G}{6H^2} (\rho + 3P)$$

$$= \frac{1}{6H^2} \left( -4 \times \frac{1}{2} G_{ij} \dot{\varphi}^i \dot{\varphi}^j + 2U \right). \quad (\text{A6})$$

It can be easily seen that the equation of state parameter  $\omega = P/\rho$  and parameter  $q$  are linearly connected:

$$q = -\frac{1}{2}(1 + 3\omega). \quad (\text{A7})$$

From the definition of the acceleration parameter, it follows that  $q$  is constant in the case of the power law and de Sitter-like behavior

$$q = \begin{cases} (s-1)/s; & a \propto t^s, \\ 1; & a \propto e^{Ht}. \end{cases} \quad (\text{A8})$$

For example,  $q = -0.5$  during the matter dominated (MD) stage, where  $s = 2/3$ .

Because the minisuperspace metric  $G_{ij}$  is flat, the scalar field equations are

$$\ddot{\varphi}^i + 3H\dot{\varphi}^i + G^{ij} \frac{\partial U}{\partial \varphi^j} = 0. \quad (\text{A9})$$

For the action (A1), the corresponding Hamiltonian is

$$\mathcal{H} = \frac{8\pi G}{2a^3} G^{ij} P_i P_j + \frac{a^3}{8\pi G} U, \quad (\text{A10})$$

where

$$P_i = \frac{a^3}{8\pi G} G_{ij} \dot{\varphi}^j \quad (\text{A11})$$

are the canonical momenta, and equations of motion have also the canonical form

$$\dot{\varphi}^i = \frac{\partial \mathcal{H}}{\partial P_i}, \quad \dot{P}_i = -\frac{\partial \mathcal{H}}{\partial \varphi^i}. \quad (\text{A12})$$

It can be easily seen that the latter equation (for  $\dot{P}_i$ ) is equivalent to the Eq. (A9).

Thus, the Friedmann equations together with the scalar field equations can be replaced by the system of the first-order ODEs

$$\dot{\varphi}^i = \frac{8\pi G}{a^3} G^{ij} P_j, \quad (\text{A13})$$

$$\dot{P}_i = -\frac{a^3}{8\pi G} \frac{\partial U}{\partial \varphi^i}, \quad (\text{A14})$$

$$\dot{a} = aH, \quad (\text{A15})$$

$$\dot{H} = \frac{\ddot{a}}{a} - H^2 = \frac{1}{6} \left( -4 \times \frac{1}{2} G_{ij} \dot{\varphi}^i \dot{\varphi}^j + 2U \right) - H^2 \quad (\text{A16})$$

with Eq. (A4) considered in the form of the initial conditions

$$H(t=0) = \sqrt{\frac{1}{3} \left( \frac{1}{2} G_{ij} \dot{\varphi}^i \dot{\varphi}^j + U \right)} \Big|_{t=0}. \quad (\text{A17})$$

We can make these equations dimensionless:

$$\frac{d\varphi^i}{M_{\text{Pl}} dt} = \frac{8\pi}{M_{\text{Pl}}^3 a^3} G^{ij} P_j, \quad \Rightarrow \frac{d\varphi^i}{dt} = \frac{8\pi}{a^3} G^{ij} P_j; \quad (\text{A18})$$

$$\frac{dP_i}{M_{\text{Pl}} dt} = -\frac{\alpha^3 M_{\text{Pl}}^3}{8\pi} \frac{\partial(U/M_{\text{Pl}}^2)}{\partial\varphi^i}, \quad \Rightarrow \frac{dP_i}{dt} = -\frac{\alpha^3}{8\pi} \frac{\partial U}{\partial\varphi^i}. \quad (\text{A19})$$

That is to say the time  $t$  is measured in the Planck times  $t_{\text{Pl}}$ , the scale factor  $a$  is measured in the Planck lengths  $L_{\text{Pl}}$ , and the potential  $U$  is measured in the  $M_{\text{Pl}}^2$  units.

We use this system of dimensionless first-order ODEs together with the initial condition (A17) for numerical calculation of the dynamics of considered models with the help of a MATHEMATICA package [36].

## APPENDIX B: SELF-SIMILARITY CONDITION

Because of the zero-minimum conditions  $U(\phi_{\min}) = f_1^2 = \lambda/2$ , the effective potential (3.1) can be written in the form

$$U_{\text{eff}}(\varphi, \phi) = U(\phi_{\min}) e^{-\sqrt{(2d_1)/(d_1+2)}\varphi} \left[ \frac{U(\phi)}{U(\phi_{\min})} + e^{-2\sqrt{(2d_1)/(d_1+2)}\varphi} - 2e^{-\sqrt{(2d_1)/(d_1+2)}\varphi} \right]. \quad (\text{B1})$$

Exact expressions for  $U(\phi)$  (3.7) and (4.2) indicate that the ratio

$$\frac{U(\phi)}{U(\phi_{\min})} = F(\phi, k, d_1) \quad (\text{B2})$$

depends only on  $\phi$ ,  $k$ , and  $d_1$ . The dimensionless parameter  $k = \xi\Lambda_D$  for the quadratic model and  $k = \gamma\Lambda_D^3$  for the quartic model. In Eq. (B2) we take into account that  $\phi_{\min}$  is a function of  $k$  and  $d_1$ :  $\phi_{\min} = \phi_{\min}(k, d_1)$ . Then,  $U(\phi_{\min})$  defined in Eqs. (3.7) and (4.2) reads as

$$U(\phi_{\min}) = \Lambda_D \tilde{F}(\phi_{\min}(k, d_1), k, d_1). \quad (\text{B3})$$

Therefore, parameters  $k$  and  $d_1$  determine fully the shape of the effective potential, and parameter  $\Lambda_D$  serves for conformal transformation of this shape. This conclusion is confirmed also in Secs. III and IV, where we show that positions of all extrema in the  $(\varphi, \phi)$  plane depend only on

$k$  and  $d_1$ . Thus, Figs. 2 and 7 for contour plots are defined by  $k$  and  $d_1$  and will not change with  $\Lambda_D$ . From the definition of the slow-roll parameters it is clear that they also do not depend on the height of potentials, and in our model depend only on  $k$  and  $d_1$  (see Figs. 8 and 9). Similar dependence takes place for the difference  $\Delta\phi = \phi_{\max} - \phi_{\min}$  drawn in Fig. 13. Thus, the conclusions concerning the slow-roll and topological inflations are fully determined by the choice of  $k$  and  $d_1$  and do not depend on the height of the effective potential, in other words, on  $\Lambda_D$ . So, for the fixed  $k$  and  $d_1$  parameter  $\Lambda_D$  can be arbitrary. For example, we can take  $\Lambda_D$  in such a way that the height of the saddle point  $\chi_{2(+)}$  will correspond to the restriction on the slow-roll inflation potential (see, e.g., [43])  $U_{\text{eff}} \lesssim 2.2 \times 10^{-11} M_{\text{Pl}}^4$ , or in our notations  $U_{\text{eff}} \lesssim 5.5 \times 10^{-10} M_{\text{Pl}}^2$ .

Above, we indicate figures that (for given  $k$  and  $d_1$ ) do not depend on the height of the effective potential (on  $\Lambda_D$ ). What will happen with dynamical characteristics drawn in Figs. 10–12 (and analogous ones for the quadratic model) if we, keeping fixed  $k$  and  $d_1$ , will change  $\Lambda_D$ ? In other words, we keep the positions of the extrema points (in  $(\varphi, \phi)$ -plane) but change the height of the extrema. We can easily answer this question using the self-similarity condition of the Friedmann equations. Let the potential  $U$  in Eqs. (A2) and (A3) be transformed conformally:  $U \rightarrow cU$ , where  $c$  is a constant. Next, we can introduce a new time variable  $\tau := \sqrt{c}t$ . Then, from Eqs. (A2)–(A5) it follows that the Friedmann equations have the same form as for the model with potential  $U$ , where time  $t$  is replaced by time  $\tau$ . We call this condition the self-similarity. Thus, if in our model we change the parameter  $\Lambda_D$ :  $\Lambda_D \rightarrow c\Lambda_D$ , it results (for fixed  $k$  and  $d_1$ ) in a rescaling of all dynamical graphics (e.g., Figs. 10–12) along the time axis in  $1/\sqrt{c}$  times (a decrease of  $\Lambda_D$  leads to a stretching of these figures along the time axis and *vice versa* an increase of  $\Lambda_D$  results in a shrinking of these graphics). The numerical calculations confirm this conclusion. The property of the conformal transformation of the shape of  $U_{\text{eff}}$  with change of  $\Lambda_D$  for fixed  $k$  and  $d_1$  can be also called as the self-similarity condition.

[1] H. V. Peiris *et al.*, *Astrophys. J. Suppl. Ser.* **148**, 213 (2003).  
 [2] M. Rainer and A. Zhuk, *Gen. Relativ. Gravit.* **32**, 79 (2000).  
 [3] U. Günther and A. Zhuk, *Phys. Rev. D* **56**, 6391 (1997).  
 [4] R. Kallosh, N. Sivanandam, and M. Soroush, *Phys. Rev. D* **77**, 043501 (2008).  
 [5] A. Linde and A. Westphal, *J. Cosmol. Astropart. Phys.* **03** (2008) 005.

[6] J. P. Conlon, R. Kallosh, A. Linde, and F. Quevedo, *J. Cosmol. Astropart. Phys.* **09** (2008) 011.  
 [7] U. Günther and A. Zhuk, *Phys. Rev. D* **61**, 124001 (2000).  
 [8] T. P. Sotiriou and V. Faraoni, arXiv:0805.1726.  
 [9] R. P. Woodard, *Lect. Notes Phys.* **720**, 403 (2007).  
 [10] S. Nojiri and S. D. Odintsov, arXiv:0807.0685.  
 [11] U. Günther, A. Zhuk, V. B. Bezerra, and C. Romero, *Classical Quantum Gravity* **22**, 3135 (2005).  
 [12] A. A. Starobinsky, *Phys. Lett.* **91B**, 99 (1980).

- [13] U. Günther, P. Moniz, and A. Zhuk, Phys. Rev. D **66**, 044014 (2002).
- [14] K. A. Bronnikov and S. G. Rubin, Grav. and Cosmol. **13**, 253 (2007).
- [15] J. Ellis, N. Kaloper, K. A. Olive, and J. Yokoyama, Phys. Rev. D **59**, 103503 (1999).
- [16] A. Linde, Phys. Lett. B **327**, 208 (1994).
- [17] T. Appelquist, H.-C. Cheng, and B. A. Dobrescu, Phys. Rev. D **64**, 035002 (2001); E. Ponton and E. Poppitz, J. High Energy Phys. 06 (2001) 019; H.-C. Cheng, K. T. Matchev, and M. Schmaltz, Phys. Rev. D **66**, 036005 (2002); G. Servant and T. M. P. Tait, Nucl. Phys. **B650**, 391 (2003); L. Bergstrom, T. Bringmann, M. Eriksson, and M. Gustafsson, Phys. Rev. Lett. **94**, 131301 (2005); F. De Fazio, arXiv:hep-ph/0609134.
- [18] P. K. Townsend, arXiv:hep-th/9612121; J. W. Moffat, arXiv:hep-th/0111225.
- [19] A. Kundu, arXiv:0806.3815.
- [20] P. G. O. Freund and M. A. Rubin, Phys. Lett. **97B**, 233 (1980).
- [21] U. Günther, P. Moniz, and A. Zhuk, Phys. Rev. D **68**, 044010 (2003).
- [22] A. Zhuk, in *Proceedings of the 14th International Seminar on High Energy Physics "QUARKS-2006" in St. Petersburg, 2006* (INR Press, St. Petersburg, 2007), Vol. 2, p. 264.
- [23] B. Ratra and P. J. Peebles, Phys. Rev. D **37**, 3406 (1988).
- [24] G. F. R. Ellis and M. S. Madsen, Classical Quantum Gravity **8**, 667 (1991).
- [25] B. Ratra, Phys. Rev. D **45**, 1913 (1992).
- [26] C. Stornaiolo, Phys. Lett. A **189**, 351 (1994).
- [27] N. Sakai, H. Shinkai, T. Tachizawa, and K. Maeda, Phys. Rev. D **53**, 655 (1996); **54**, 2981(E) (1996).
- [28] T. Saidov and A. Zhuk, Phys. Rev. D **75**, 084037 (2007).
- [29] N. Arkani-Hamed, S. Dimopoulos, and J. March-Russell, Phys. Rev. D **63**, 064020 (2001).
- [30] U. Günther, A. Starobinsky, and A. Zhuk, Phys. Rev. D **69**, 044003 (2004).
- [31] Y. M. Cho and Y. Y. Keum, Classical Quantum Gravity **15**, 907 (1998).
- [32] Y. M. Cho and J. H. Kim, arXiv:0711.2858.
- [33] J. Martin and D. Schwarz, Phys. Rev. D **62**, 103520 (2000).
- [34] N. Deruelle, M. Sasaki, and Y. Sendouda, Phys. Rev. D **77**, 124024 (2008).
- [35] T. T. Nakamura and E. D. Stewart, Phys. Lett. B **381**, 413 (1996); J.-O. Gong and E. D. Stewart, Phys. Lett. B **538**, 213 (2002).
- [36] R. Kallosh and S. Prokushkin, arXiv:hep-th/0403060.
- [37] D. H. Lyth and A. Riotto, Phys. Rep. **314**, 1 (1999); G. Efstathiou and K. J. Mack, J. Cosmol. Astropart. Phys. 05 (2005) 008.
- [38] H. V. Peiris and R. Easther, J. Cosmol. Astropart. Phys. 07 (2008) 024.
- [39] T. Saidov and A. Zhuk, Gravitation Cosmol. **12**, 253 (2006).
- [40] A. Vilenkin, Phys. Rev. Lett. **72**, 3137 (1994).
- [41] A. R. Liddle and D. H. Lyth, Phys. Rep. **231**, 1 (1993).
- [42] G. Barenboim and O. Vives, arXiv:0806.4389.
- [43] D. H. Lyth, Phys. Lett. **147B**, 403 (1984).